Soliton model of the crystalline α relaxation

Jia-Lin Syi* and Marc L. Mansfield†
Department of Chemical and Nuclear Engineering, University of Maryland, College Park, Maryland 20742, USA; and Michigan Molecular Institute, 1910 West St Andrews Road, Midland, Michigan 48640, USA
(Received 11 May 1987; revised 26 October 1987; accepted 18 November 1987)

In an effort to extend the successful soliton model of the α relaxation of crystalline polyethylene to other crystalline polymers, solitons producing net rotation and/or translation of crystalline polymer stems are studied for four polymers: polyethylene, isotactic and syndiotactic polypropylene, and isotactic polystyrene. We are able successfully to predict the activation energy of the α relaxation in both polyethylene and isotactic polypropylene, and to explain the absence of the α relaxation in both syndiotactic polypropylene and isotactic polystyrene. Criteria controlling the absence or presence of the α relaxation in any particular polymer crystal are: first, the energy barrier opposing motion of each individual repeat unit of the stem; secondly, the elongational stiffness of the polymer stem; and thirdly, the number of bonds per repeat unit. The stems in thin polyethylene or paraffin crystals are predicted to support both rigid-rod translations and a combined rotation–translation soliton.

(Keywords: α relaxation; solitons; crystal motion)

INTRODUCTION

The potential energy exerted by the surrounding crystalline stems upon a given stem in a polymer crystal reflects, of course, the symmetry of the stem. For example, a complete rotation of the stem through 360° brings it back into crystallographic register, as does a translation along the fibre axis through the unit-cell dimension. In addition, because the polymer stem is helical, other symmetry-preserving transformations, namely screwing the helix in or out of the crystal, can also be considered. Examples of these are a combined 180° rotation and $c/2$ translation in polyethylene, and a combined 120° rotation and $c/3$ translation in isotactic polypropylene, where c in either case represents the unit-cell dimension along the fibre axis. In either case, the polymer stem finds itself moved forwards or back by one chemical repeat unit. One could consider motions within the crystal in which a stem jumps from a particular minimum energy position in the lattice to some other symmetry-equivalent position through a combined translation–rotation motion as a rigid rod. Such rigid-rod motions probably occur in thin crystals (see below), but since they require an activation barrier proportional to the crystal thickness, a motion in which the polymer stem moves flexibly between symmetry-equivalent positions is preferred in thick crystals. In thick crystals, motions having activation barriers independent of crystal thickness can occur if one end of the stem makes the transition, followed by the remaining portions of the stem at later times as a distorted region travels along the stem.

Such a combined rotation–translation motion travelling along the stem has been considered as the mechanism of the α relaxation of polyethylene for quite some time[1-7]. In 1978, the energy and structure of the distorted region were calculated, and they were found to be in good agreement with the activation energy and relaxation frequency as a function of crystal thickness over a wide range of thicknesses[8]. In 1980[9-11] it was pointed out that the motion is a particular example of a class of non-linear waves, a so-called soliton or solitary wave[12]. Finally, Skinner and Park[13] showed in 1984 that the soliton model could predict dielectric relaxation curves in polyethylene over a wide range of frequencies and temperatures, providing, so far as we know, the only successful molecular model of a polymer relaxation. For more details, the reader is referred to the reviews by Boyd[14,15].

The distorted region in polyethylene combines a twist about the stem axis through 180° and an accumulated translational distortion parallel to the chain axis of half the unit-cell dimension. The twist is predicted[8] to occupy about 12 bonds, with each bond distorted an average of about 15° away from the *trans* rotational state, while the translational distortion extends over roughly 100 bonds and in thick crystals leads to a compression or expansion of the stem by one CH_2 group. The motion leads to dielectric relaxation by being created thermally at one face and travelling through to the other, leaving the stem translated along its axis by one CH_2 group and rotated through 180° relative to its original position.

We show below that any polymer crystallizing in a helical structure has sufficient symmetry to support soliton solutions to its equation of motion, requiring only a set of symmetry-equivalent minimum energy positions for each stem. However, the α relaxation has been observed in only a handful of polymers[14,15]. If the soliton mechanism is valid for all polymers exhibiting an α relaxation, it should explain the presence or absence of an α relaxation in any particular case. To understand better the factors

* Present address: National Institutes of Health, Bethesda, Maryland 20892, USA
† To whom enquiries should be addressed at Michigan Molecular Institute

0032-3861/88/060987-11$03.00

controlling the existence of the α relaxation, we have computed the structures and energies of solitons in four different polymer crystals, namely, polyethylene (PE) and isotactic polypropylene (iPP), both exhibiting an α relaxation[14,15], and isotactic polystyrene (iPS) and syndiotactic polypropylene (sPP)[16], for which no α relaxation has been observed. These calculations give a better understanding of the factors leading to the α relaxation.

The approach employed here to calculate soliton structures and energies is similar to the Mansfield–Boyd calculation for polyethylene[8], but, owing to limitations in computational resources, is more crude. For this reason, the calculation of the polyethylene soliton given below is not an improvement on the Mansfield–Boyd calculation. It was done to permit a comparison between the crude approach employed here and the more precise calculation. A number of interesting results have been obtained in spite of the crudity of our calculation.

The soliton equation of motion employed in this paper has been derived elsewhere[9], and is discussed in the second section. In the third section, we describe the computational approach employed in this paper. In the fourth section we derive expressions for two quantities required by the model, namely, spring constants characterizing the translational and rotational stiffness of a particular polymer stem. In the fifth section we present the results of these calculations for each of the four polymers named above. In the sixth section we summarize our results, discussing the properties that control the presence of the α relaxation.

SOLITON EQUATION OF MOTION

Elsewhere[9] we have derived the following equations to describe the motion of a crystalline stem:

$$\frac{\partial^2 x}{\partial z^2}-\frac{1}{c_1^2}\frac{\partial^2 x}{\partial t^2}=\frac{1}{k_1 l^2}\frac{\partial U}{\partial x} \tag{1a}$$

$$\frac{\partial^2 \theta}{\partial z^2}-\frac{1}{c_2^2}\frac{\partial^2 \theta}{\partial t^2}=\frac{1}{k_2 l^2}\frac{\partial U}{\partial \theta} \tag{1b}$$

These represent the equations of motion of a continuum model of a single polymer stem in which it is assumed that the position of each repeat unit in the stem is determined by two variables, a displacement along the stem axis and a rotation about the axis. In these equations, l is the distance between repeat units along the stem in a perfect crystal, t is the time, z is the position that the repeat unit would assume in the perfect crystal, $x(z,t)$ gives the displacement of the repeat unit with perfect-crystal position z away from its perfect-crystal position, and $\theta(z,t)$ is the rotation of the repeat unit away from its perfect-crystal position. $U(x,\theta)$ is the potential felt by a given repeat unit due to neighbouring stems. In deriving equations (1) it is assumed that the relative displacements of adjacent repeat units are sufficiently small that the potential energy contributed from within the stem is entirely harmonic in the relative displacements of adjacent repeat units. The spring constants k_1 and k_2 determine these harmonic functions for the translational and rotational displacements, respectively. The quantities $c_i=k_i l^2/m_i$, for m_1 the mass and m_2 the moment of inertia, respectively, of a repeat unit, are the velocities of low-amplitude longitudinal and transverse sound waves, respectively.

The coordinate transformation

$$\xi=z-vt \tag{2}$$

transforms from the laboratory reference frame to a reference frame moving with velocity v parallel to the stem. Equations (1) are transformed to:

$$\frac{\partial^2 x}{\partial \xi^2}=\frac{\gamma_1^2}{k_1 l^2}\frac{\partial U}{\partial x} \tag{3a}$$

$$\frac{\partial^2 \theta}{\partial \xi^2}=\frac{\gamma_2^2}{k_2 l^2}\frac{\partial U}{\partial \theta} \tag{3b}$$

where

$$\gamma_i^2=(1-v^2/c_i^2)^{-1} \tag{4}$$

We have been unable to write down a solution that is valid for arbitrary $U(x,\theta)$. However, a qualitative understanding of a particular class of solutions is not difficult to obtain. Consider solutions such that x and θ at $\xi\rightarrow+\infty$ take on values for which U is at a minimum, while at $\xi\rightarrow-\infty$, x and θ lie at a different, but symmetry-equivalent, minimum of U. Since the equations of motion lose all explicit time dependence in the moving reference frame, we conclude that the solution maintains a constant profile in time. The velocity is arbitrary, constrained only by the requirement that v^2 be less than the smaller of c_1^2 or c_2^2. Note that equations (3) have the same form, up to a multiplicative factor, as equations (1) if we drop the time derivatives from the latter. This implies that the dynamic problem is solved automatically by solving a static force (and torque) balance problem with modified values of the spring constants:

$$k_i\rightarrow k_i/\gamma_i^2 \tag{5}$$

We have no real difficulty imagining the form of the solution to the static force balance problem: the two ends of the stem lie in different but symmetry-equivalent minimum energy positions separated by a strained region whose structure is dictated by the details of the force balance. We conclude that the equations of motion predict the existence of a wave pulse, moving down the stem with constant shape, which transfers chain segments between two symmetry-equivalent minimum energy positions as it passes.

Any localized wave pulse travelling with constant profile is called a solitary wave[12]. We have shown above that solutions to equations (1) exist that fit this definition. The term 'soliton' denotes solitary waves that preserve their shape and velocity in collisions[12]. Similar wave equations are known to have this property (e.g. the sine–Gordon and ϕ^4 solitons[12]) and solutions to equations (1) probably do, too. Nevertheless, we have not investigated any multiple-soliton solutions to equations (1), so that our use of the term 'soliton' is not rigorously justified. Given the energy required to create a single soliton in these systems, two-soliton interactions should be too infrequent to be of any physical significance, so that the question is not an important one.

These solitons carry conserved energy, conserved linear momentum and conserved angular momentum[12]. The total kinetic and potential energies, respectively, carried by the solitons are given by the integrals:

$$T=\frac{1}{2l}\int_{-\infty}^{+\infty} dz\left[m_1\left(\frac{\partial x}{\partial t}\right)^2+m_2\left(\frac{\partial \theta}{\partial t}\right)^2\right] \quad (6a)$$

$$=\frac{v^2}{2l}\int_{-\infty}^{+\infty} d\xi\left[m_1\left(\frac{\partial x}{\partial \xi}\right)^2+m_2\left(\frac{\partial \theta}{\partial \xi}\right)^2\right] \quad (6b)$$

$$V=\int_{-\infty}^{+\infty} dz\left[\frac{k_1 l}{2}\left(\frac{\partial x}{\partial z}\right)^2+\frac{k_2 l}{2}\left(\frac{\partial \theta}{\partial z}\right)^2+\frac{U}{l}\right] \quad (7a)$$

$$=\int_{-\infty}^{+\infty} d\xi\left[\frac{k_1 l}{2}\left(\frac{\partial x}{\partial \xi}\right)^2+\frac{k_2 l}{2}\left(\frac{\partial \theta}{\partial \xi}\right)^2+\frac{U}{l}\right] \quad (7b)$$

The total linear momentum carried by the soliton is:

$$P_1=\frac{m_1}{l}\int_{-\infty}^{+\infty} dz\frac{\partial x}{\partial t}=\frac{-m_1 v}{l}\int_{-\infty}^{+\infty} d\xi\frac{\partial x}{\partial \xi}=\frac{-m_1 v}{l}\Delta x \quad (8)$$

and the total angular momentum is:

$$P_2=\frac{m_2}{l}\int_{-\infty}^{+\infty} dz\frac{\partial \theta}{\partial t}=\frac{-m_2 v}{l}\int_{-\infty}^{+\infty} d\xi\frac{\partial \theta}{\partial \xi}=\frac{-m_2 v}{l}\Delta\theta \quad (9)$$

where $\Delta x=x(+\infty)-x(-\infty)$ and $\Delta\theta=\theta(+\infty)-\theta(-\infty)$ are the total amounts by which the two stems are translated or rotated relative to one another.

Equations (1) neglect a number of dissipative mechanisms that affect the motion of the soliton, including interactions with lattice vibrations and interactions with or collapse into less mobile crystalline defects such as the Reneker defect[17,18] in polyethylene, etc. It has proved necessary to include such dissipative effects, as least phenomenologically, in the soliton model to achieve complete agreement with experiment. For example, Mansfield and Boyd[8] found it necessary to apply a soliton scattering correction in thick crystals to fit the experimental activation energy vs. crystal thickness curve, and Skinner and Park[13] obtained good fits to the dielectric dispersion curves only by including a thermally activated dissipative mechanism, with an activation energy provocatively close to the estimated Reneker defect energy, suggesting that soliton scattering or annihilation by Reneker defects is an important process. It follows that the view afforded by equations (1) of a robust soliton travelling through the crystal with no change in shape, velocity, energy, etc., is not completely correct. On the other hand, the scattering corrections are not large and the free-streaming mode of motion predicted by equations (1) is indicated by the theoretical analysis of the relevant experiments. In other words, we do not believe that these dissipative effects are strong enough to destroy completely the free-streaming behaviour predicted by the equation of motion that neglects them. Any system in which they are strong enough to suppress this motion most probably does not exhibit an α relaxation.

The potential energy carried by the soliton is constant only in the continuum limit. Since the continuum model is only an idealization, we expect the potential energy to vary periodically as the soliton advances from one unit cell to the next. This variation in potential energy should contribute to soliton scattering, becoming more important as the continuum approximation becomes less valid. If these potential energy ripples ever become comparable to $k_B T$, the free-streaming motion of the soliton is probably impossible. Any such polymers would not have an α relaxation. In this paper, we estimate the height of these ripples in each of the polymers.

COMPUTATIONAL DETAILS

We have employed a finite-differences technique to calculate solutions to equations (3). If the nodes in the calculation are spaced at intervals of h apart, then the finite-difference form of equations (3) is:

$$k_1'(x_{j+1}-2x_j+x_{j-1})=\gamma_1^2 U_x'(x_j,\theta_j) \quad (10a)$$

$$k_2'(\theta_{j+1}-2\theta_j+\theta_{j-1})=\gamma_2^2 U_\theta'(x_j,\theta_j) \quad (10b)$$

where

$$k_1'=(l/h)k_i \qquad U'(x,\theta)=(h/l)U(x,\theta) \quad (11)$$

and the subscripts x or θ denote differentiation with respect to x or θ, respectively. *Table 1* gives the values of l, h and the spring constants employed in this calculation. We chose values of h equal to the average interatomic distance along the backbone, so that l/h is equal to the number of backbone atoms per repeat unit. Equations (10) were solved by a standard Newton–Raphson technique. The total potential energy was then computed as:

$$V=\tfrac{1}{2}\sum_j[k_1'(x_j-x_{j-1})^2+k_2'(\theta_j-\theta_{j-1})^2+2U'(x_j,\theta_j)] \quad (12)$$

The present model is completely specified by assigning values for k_1, k_2 and the function $U(x,\theta)$. In the next section we explain how we estimated k_1 and k_2. Estimates for U and its derivatives were obtained in the following way. One crystalline stem surrounded by its near neighbours was constructed according to crystal structure parameters found in the literature.* This stem was permitted to move about within the environment of the neighbouring stems, which were held rigid. *Figure 1* shows the moving and stationary stems used in this calculation for each of the four polymers. We considered all possible pairings of atoms between a single repeat unit of the moving chain and all atoms in the neighbouring stems out to a distance of 15 Å. The contribution to U from each atomic pair was taken as $Ae^{-Br}-C/r^6$ for r the interatomic distance and with different A, B and C parameters for carbon–carbon, carbon–hydrogen and

* The polyethylene crystal structure was taken to be the same as in ref. 8. The crystal structures of the other three polymers were taken from ref. 19.

Table 1 Values of some parameters[a] used in this calculation

Polymer	c (Å)	l (Å)	h (Å)	k_1 (kcal mol^{-1})	k_2 (kcal mol^{-1} Å^{-2})	k'_1 (kcal mol^{-1})	k'_2 (kcal mol^{-1} Å^{-2})
PE	2.548	1.274	1.274	28.4	361.2	28	361
iPP	6.35	2.12	1.06	17.0	52.2	34	104
sPP	7.07	3.54	0.88	11.4	8.3	46	33
iPS	6.65	2.22	1.11	17.0	52.2	34	104

[a] c is the unit-cell dimension along the stem axis; l is the length per repeat unit along the stem axis; h is the node interval in the finite-difference solution of the equation of motion, set equal to length per backbone bond along the helix axis; k_1 and k'_1 are twisting spring constants for a repeat unit and a backbone bond, respectively; and k_2 and k'_2 are stretching spring constants for a repeat unit and a backbone bond, respectively

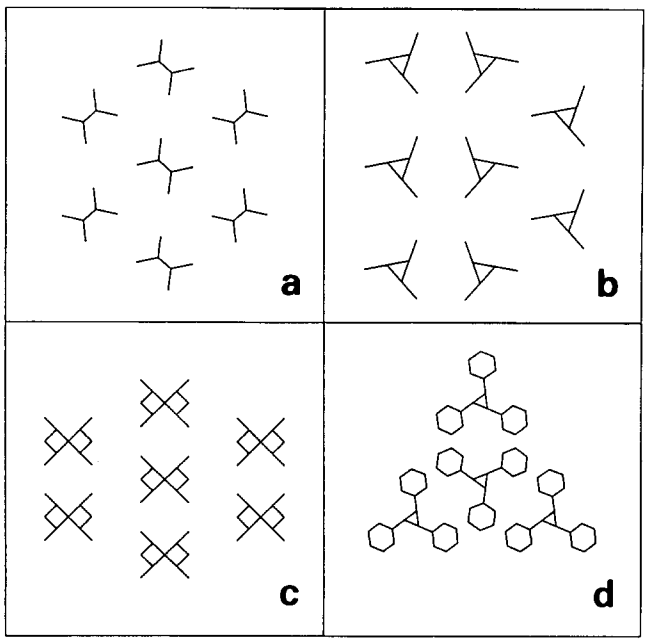

Figure 1 Schematic diagram of structures used to calculate the interstem potential energy function $U(x,\theta)$: (a) polyethylene; (b) isotactic polypropylene; (c) syndiotactic polypropylene; (d) isotactic polystyrene. The central stem was rotated and translated in the crystal field of the other stems, which were held rigid. Contributions from the stems shown only were included

hydrogen–hydrogen pairs. The parameters A, B and C used were those given by Shieh *et al.*[20] and U was calculated in this way at a set of grid points (spaced every 10° in θ and at intervals of $c/20$ in x) for a complete rotation through 360° and a complete translation through c, where c represents the unit-cell dimension. A Fourier series, given in *Table 2*, was then developed for polyethylene that is accurate at almost all values of x and θ to within about 0.1 kcal mol^{-1}. Satisfactory Fourier series could not be obtained for any of the other polymers, and so a spline interpolation procedure described in ref. 21 was employed. Both the Fourier series for polyethylene and the spline interpolation for the other polymers have continuous first and second derivatives, which is of paramount importance for the convergence of the Newton–Raphson iteration. Contour plots of the functions $U'(x,\theta)=(h/l)U(x,\theta)$ for the four polymers are shown in *Figures 2–5*. McCullough[22] has also calculated such functions for polyethylene.

Table 3 lists the minima in either the Fourier series approximation or the spline interpolation approximation of each U' function. *Table 3* indicates that the spline interpolation disrupts the exact symmetry of the U'

Table 2 Fourier series approximation[a] of U' for polyethylene

Coefficient	θ dependence	x dependence
0.585698	1	1
−0.044695	C2	1
−0.350311	C4	1
0.041593	S2	1
−0.152897	S4	1
−0.264431	C1	C2
−0.007697	C3	C2
0.072608	C5	C2
0.201464	S1	C2
0.131279	S3	C2
−0.058807	S5	C2
0.005141	1	C4
0.000544	C1	S2
0.000030	S1	S2
−0.000244	1	S4

[a] Cn and Sn in the θ-dependence column represent $\cos(n\theta)$ and $\sin(n\theta)$, respectively. Cn and Sn in the x-dependence column represent $\cos(n\pi x/c)$ and $\sin(n\pi x/c)$, respectively, for $c=2.548$ Å

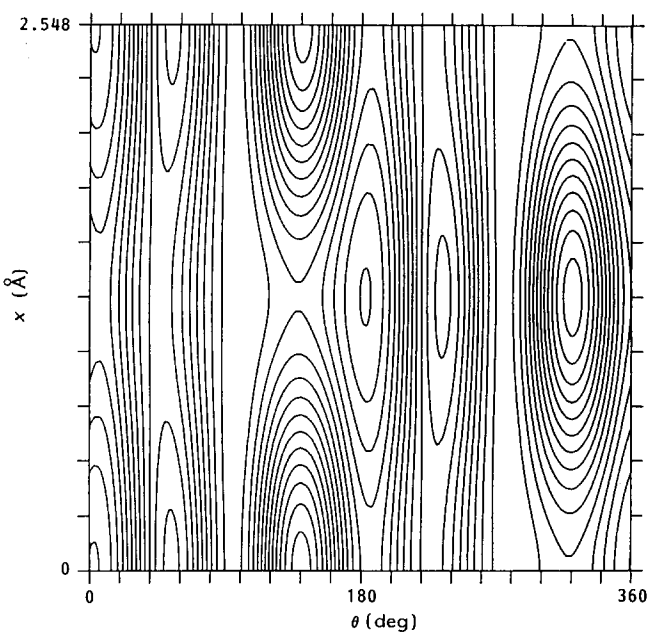

Figure 2 Contour plot of the function $U'(x,\theta)$ for polyethylene. Contours are drawn at intervals of 0.1 kcal mol^{-1} (see also *Figure 7*)

function since minima expected to have equal energies differ slightly. The lack of exact symmetry is also apparent in some of the contour plots in *Figures 3–5*. This lack of complete symmetry is not expected to be important given the level of accuracy of these calculations.

The spline interpolation has the defect of having

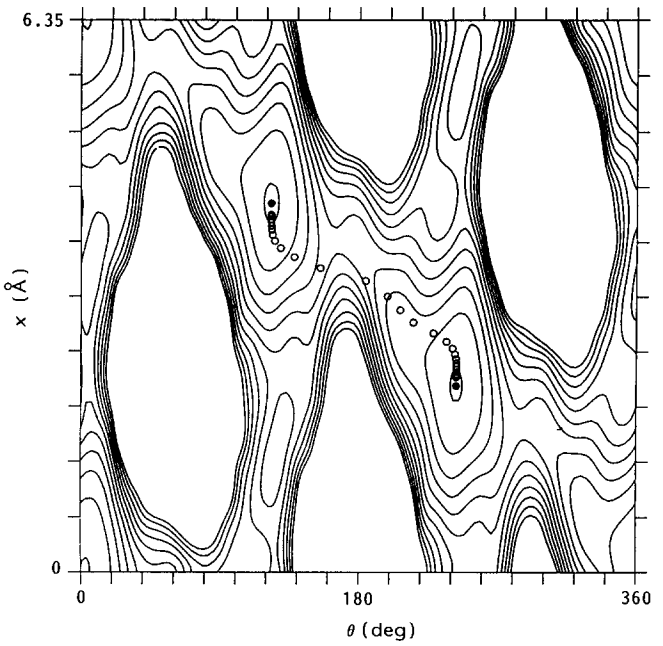

Figure 3 Contour plot of the function $U'(x,\theta)$ for isotactic polypropylene. Contours are drawn at intervals of 1 kcal mol^{-1}, and contours above 10 kcal mol^{-1} have been omitted for clarity. Closed circles give the positions of the minima of $U'(x,\theta)$. Open circles give the computed soliton structure

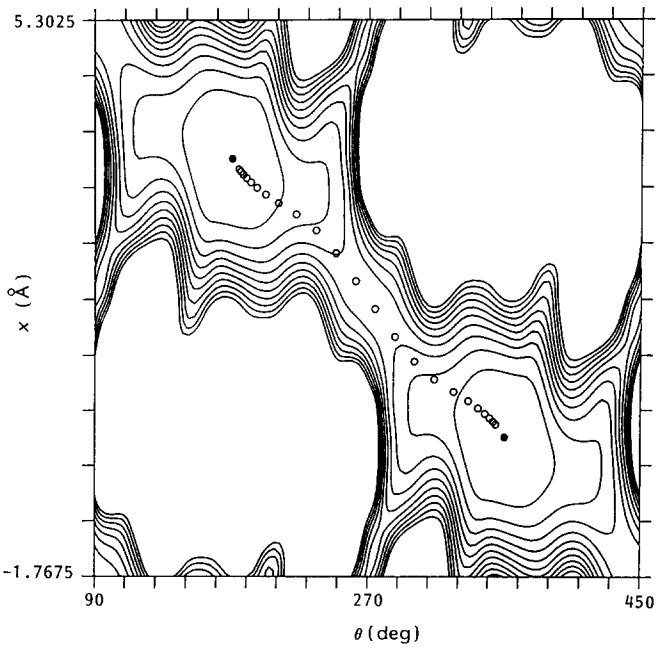

Figure 4 Contour plot of the function $U'(x,\theta)$ for syndiotactic polypropylene. Contours are drawn at intervals of 1 kcal mol^{-1}, and contours above 10 kcal mol^{-1} have been omitted for clarity. Closed circles give the positions of the minima of $U'(x,\theta)$. Open circles give the computed soliton structure

discontinuous derivatives at the boundary of the plot. The function itself is continuous upon going from one side of the plot to the other, but not its derivatives. Therefore, convergence of the Newton–Raphson iteration procedure is difficult, if not impossible, near the boundaries. These problems are avoided by a simple shift of the boundaries whenever the soliton finds itself close to the boundary. For this reason, the syndiotactic polypropylene plot has θ varying from $\pi/4$ to $5\pi/4$, and x from -1.7675 to 5.3025 Å. Of course, the Fourier series approximation of polyethylene has no continuity problems and convergence is possible even when the soliton crosses the boundary.

For a number of reasons (to be discussed below), it was necessary to apply constraints to certain of the x_j or θ_j variables in some calculations. Constraints of the general form x_j = constant or θ_j = constant were applied through the use of Lagrange multipliers.

One useful property of equations (10) is that coupling only extends to nearest neighbours. In other words, x_j is coupled only to $x_{j\pm1}$, to θ_j and to a Lagrange multiplier (if defined); while θ_j couples only to $\theta_{j\pm1}$, to x_j and possibly to a Lagrange multiplier. It follows that, by a proper ordering of the vector of independent variables (namely, $x_1, \theta_1, x_2, \theta_2, \ldots, x_j, \theta_j, \ldots$, with interdigitation of any defined Lagrange multipliers), the Newton–Raphson calculation requires a Gauss–Jordan elimination of a banded matrix, which can be performed in relatively modest times and with relatively modest memory requirements. Both computation time and required memory are proportional to N, not N^2, for N the number of degrees of freedom. We were able to obtain well converged solutions rapidly even with as many as 600 degrees of freedom.

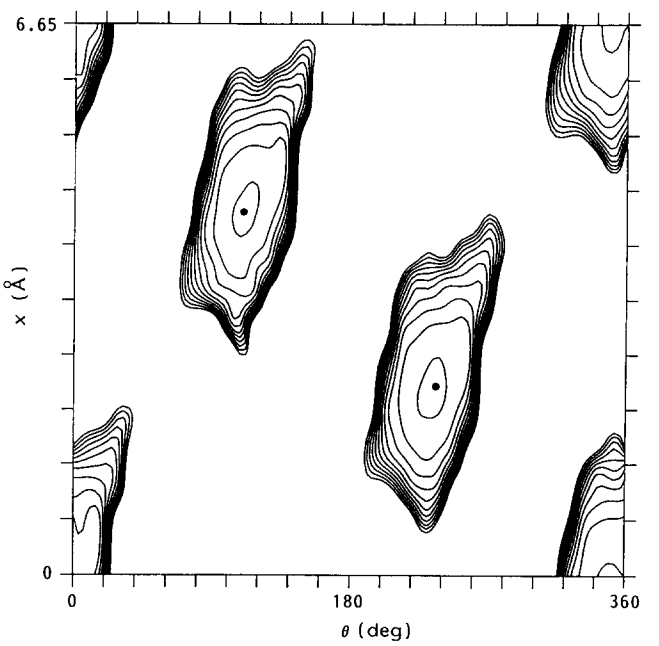

Figure 5 Contour plot of the function $U'(x,\theta)$ for isotactic polystyrene. Contours are drawn at intervals of 1 kcal mol^{-1}, and contours above 10 kcal mol^{-1} have been omitted for clarity. Closed circles give the positions of the minima of $U'(x,\theta)$

Table 3 Minima of the $U'(x,\theta)$ functions

Polymer	x (Å)	θ (deg)	$U'(x,\theta)$ (kcal mol^{-1})
PE	0	2.8	−0.009
	1.27	182.8	−0.009
iPP	0	3.0	−0.030
	2.14	243.0	−0.054
	4.25	123.2	−0.084
sPP	0	0.2	0.007
	3.54	179.8	0
iPS	2.30	235.8	−0.178
	4.38	110.0	−0.100
	6.59	348.6	−0.081

COMPUTATION OF SPRING CONSTANTS

In this section we compute the spring constants k_1 and k_2 appearing in the equations of motion. Consider a section of the polymer helix, shown schematically in *Figure 6a*. We define two 'virtual' bonds extending from the end atoms to the helix axis and lying normal to the axis as in *Figure 6a*. The spring constants k_1 and k_2 will be determined by distorting the helical section through the application of forces to the virtual bonds. The virtual bonds are employed so that the tension or torque applied to the helical section is taken along or about the helical axis. We assume that each backbone bond has stretching spring constant κ_b, that the virtual bonds have stretching spring constant κ_b', that the bond angles have bending spring constants κ_θ, that the bond angles between virtual and real bonds have bending spring constants κ_θ', and that torsion about the bonds obeys a harmonic function with spring constant κ_ϕ. We also assume that the virtual bonds are very stiff, i.e. $\kappa_b', \kappa_\theta' \to \infty$. The origin lies at the intersection of the helix axis and the first virtual bond. The intersection of the second virtual bond and the helix axis lies at the vector position $\boldsymbol{R}$. The true end of the helical section, the last atom, lies at vector position $\boldsymbol{r}$, so that $\boldsymbol{R}-\boldsymbol{r}$ represents the last virtual bond. We let $\boldsymbol{e}_3$ be the unit vector parallel to the helix axis, so that $\boldsymbol{R}=R_0\boldsymbol{e}_3$, with R_0 representing the undistorted length. Then we define $\boldsymbol{e}_1$ parallel to the last virtual bond as shown and $\boldsymbol{e}_2$ so that the triad $(\boldsymbol{e}_1,\boldsymbol{e}_2,\boldsymbol{e}_3)$ forms a mutually orthonormal set of basis vectors. Then we may write that $\boldsymbol{r}=x\boldsymbol{e}_1+R_0\boldsymbol{e}_3$, for x the distance of the last atom from the helix axis. The total energy of this helical section is:

$$U=\tfrac{1}{2}\sum_i \kappa_i(q_i-q_i^0)^2 \tag{13}$$

Here each κ_i represents one of the κ_b, κ_θ, etc., spring constants and q_i represents one of the degrees of freedom (bond length, bond angle, torsional angle). The sum extends over all degrees of freedom in the helical section. Also q_i^0 is the undistorted value of the particular q_i. We distort the helix by setting $\boldsymbol{R}=(R_0+\delta)\boldsymbol{e}_3$, and we minimize U subject to the constraint $\boldsymbol{R}=(R_0+\delta)\boldsymbol{e}_3$. This yields equations of the form:

$$0=\kappa_i(q_i-q_i^0)+\underset{\sim}{\lambda}\cdot(\partial \boldsymbol{r}_N/\partial q_i) \tag{14}$$

where $\underset{\sim}{\lambda}$ is the vector of Lagrange multipliers or the force required to maintain the displacement. Therefore

$$\underset{\sim}{\lambda}=k_{st}\delta\boldsymbol{e}_3 \tag{15}$$

and

$$U=\tfrac{1}{2}k_{st}\delta^2 \tag{16}$$

where k_{st} represents a force constant for stretching the entire helical section. Equating equations (16) and (13), inserting the expression for $(q_i-q_i^0)$ obtained from equation (14) and rearranging yields the following approximation for k_{st}:

$$k_{st}^{-1}=\sum_i \kappa_i^{-1}[\boldsymbol{e}_3\cdot(\partial\boldsymbol{R}/\partial q_i)]^2 \tag{17}$$

giving contributions from each degree of freedom to the spring constant k_{st}.

The contribution to equation (17) due to bond b_i is given by the derivative $\partial\boldsymbol{R}/\partial b_i=\boldsymbol{v}_i$ for $\boldsymbol{v}_i$ a unit vector parallel to bond i. Equation (17) then indicates that each bond contributes:

$$\kappa_b^{-1}v_{i3}^2 \tag{18}$$

to k_{st}^{-1}, where $\boldsymbol{v}_i=v_{i1}\boldsymbol{e}_1+v_{i2}\boldsymbol{e}_2+v_{i3}\boldsymbol{e}_3$. The derivatives of $\boldsymbol{R}$ with respect to θ_i or ϕ_i are obtained by crossing the axis of the rotation brought about by changes in θ_i or ϕ_i into the component of $\boldsymbol{R}$ that is rotated by changing the angle[23]. For example, as shown in *Figure 6b*, changes in θ_i produce a rotation about the axis:

$$\gamma_i=|\boldsymbol{b}_i\times\boldsymbol{b}_{i+1}|^{-1}(\boldsymbol{b}_i\times\boldsymbol{b}_{i+1}) \tag{19}$$

which is just the unit vector normal to both $\boldsymbol{b}_i$ and $\boldsymbol{b}_{i+1}$. The vector $\boldsymbol{t}_i$ in *Figure 6b* is the component of $\boldsymbol{R}$ rotated by θ_i, so the derivative with respect to θ_i is:

$$\partial\boldsymbol{R}/\partial\theta_i=\gamma_i\times\boldsymbol{t}_i \tag{20}$$

Dotting this into $\boldsymbol{e}_3$ and squaring indicates that each bond angle contributes:

$$\kappa_\theta^{-1}(\gamma_{i1}t_{i2}-\gamma_{i2}t_{i1})^2 \tag{21}$$

to k_{st}^{-1}, where $\gamma_i=\gamma_{i1}\boldsymbol{e}_1+\gamma_{i2}\boldsymbol{e}_2+\gamma_{i3}\boldsymbol{e}_3$ and $\boldsymbol{t}_i=t_{i1}\boldsymbol{e}_1+t_{i2}\boldsymbol{e}_2+t_{i3}\boldsymbol{e}_3$. Note that equation (21) is independent of t_{i3}. Likewise, as seen in *Figure 6c*, changes in ϕ_i produce rotations about the axis $\boldsymbol{v}_i$, while the component of $\boldsymbol{R}$ rotated by ϕ_i is $\boldsymbol{u}_i$. Therefore,

$$\partial\boldsymbol{R}/\partial\phi_i=\boldsymbol{v}_i\times\boldsymbol{u}_i \tag{22}$$

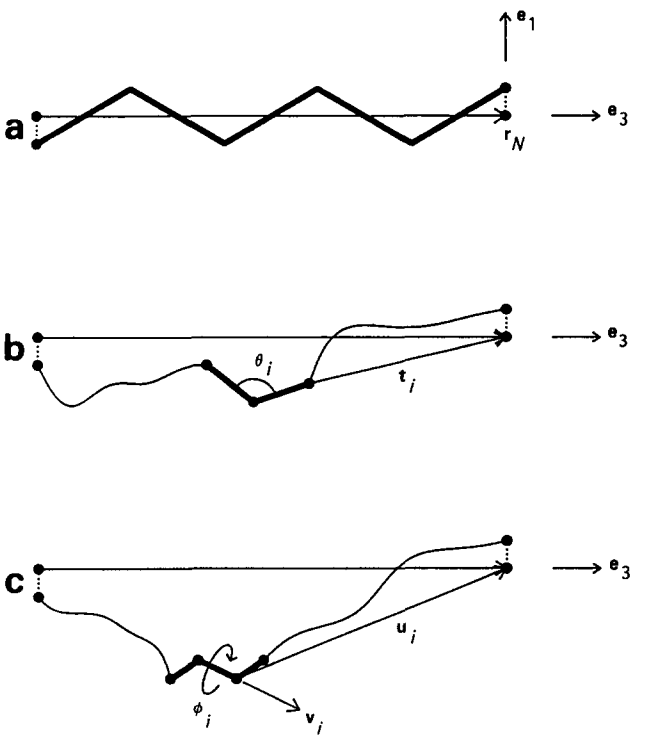

Figure 6 Diagram giving definitions of molecular parameters used in computing the chain stiffness constants k_1 and k_2. The virtual bonds discussed in the text are shown as dotted lines

and each torsional angle contributes an amount

$$\kappa_\phi^{-1}(v_{i1}u_{i2}-v_{i2}u_{i1})^2 \tag{23}$$

to k_{st}^{-1}, where $\boldsymbol{u}_i=u_{i1}\boldsymbol{e}_1+u_{i2}\boldsymbol{e}_2+u_{i3}\boldsymbol{e}_3$. Equation (23) has no u_{i3} dependence. Note that the virtual bonds make no contribution to k_{st}^{-1}.

We now derive a similar equation for k_{tw}, a spring constant for twisting the helical section. We displace $\boldsymbol{r}$ to $x\boldsymbol{e}_1+\delta\boldsymbol{e}_2+R_0\boldsymbol{e}_3$ while keeping $\boldsymbol{R}$ fixed at $\boldsymbol{R}=R_0\boldsymbol{e}_3$. This requires two Lagrange multipliers:

$$0=\kappa_i(q_i-q_i^0)+\underset{\sim}{\lambda}_1\cdot(\partial\boldsymbol{r}/\partial q_i)+\underset{\sim}{\lambda}_2\cdot(\partial\boldsymbol{R}/\partial q_i) \tag{24}$$

$\underset{\sim}{\lambda}_1$ and $\underset{\sim}{\lambda}_2$ are of equal magnitude and opposite direction:

$$\underset{\sim}{\lambda}_1=\lambda\boldsymbol{e}_2 \qquad \underset{\sim}{\lambda}_2=-\lambda\boldsymbol{e}_2 \tag{25}$$

All the following also apply:

$$U=\tfrac{1}{2}k_{tw}\Theta^2 \qquad \Theta=\delta/x \qquad k_{tw}\Theta=\lambda x \tag{26}$$

Rearranging as before yields:

$$k_{tw}^{-1}=x^{-2}\textstyle\sum_i\kappa_i^{-1}[\boldsymbol{e}_2\cdot\partial(\boldsymbol{r}-\boldsymbol{R})/\partial q_i]^2 \tag{27}$$

which becomes

$$k_{tw}^{-1}=\textstyle\sum_i\kappa_i^{-1}(\boldsymbol{e}_2\cdot\partial\boldsymbol{e}_1/\partial q_i)^2 \tag{28}$$

since $\boldsymbol{r}-\boldsymbol{R}=x\boldsymbol{e}_1$.

The contribution to equation (28) from bonds is zero, since $\partial\boldsymbol{e}_1/\partial q_1$ is zero when q_i represents a bond length. The derivative $\partial\boldsymbol{e}_1/\partial\theta_i$ is just $\underset{\sim}{\gamma}_i\times\boldsymbol{e}_1$, since $\underset{\sim}{\gamma}_i$ is the rotation axis for changes in θ_i and all of $\boldsymbol{e}_1$ is rotated by changes in θ_i. Likewise the derivative $\partial\boldsymbol{e}_1/\partial\phi_i$ is $\boldsymbol{v}_i\times\boldsymbol{e}_1$. Then each bond angle contributes an amount:

$$\kappa_\theta^{-1}\gamma_{i3}^2 \tag{29}$$

to k_{tw}^{-1}, and each torsional angle an amount:

$$\kappa_\phi^{-1}v_{i3}^2 \tag{30}$$

Note that the contributions to k_{st}^{-1} or k_{tw}^{-1} given in equations (18), (21), (23), (29) and (30) are the same for all equivalent degrees of freedom in any repeat unit. It follows that one can compute k_1^{-1} or k_2^{-1} by including contributions from just one repeat unit, and that k_{tw}^{-1} and k_{st}^{-1} are equal to nk_1^{-1} and nk_2^{-1}, respectively, for a helical sequence composed of n repeat units, as expected.

If we assume that the helices lie on the diamond lattice, the following expressions hold. For polyethylene:

$$k_1^{-1}=\tfrac{2}{3}k_\phi^{-1} \tag{31}$$

$$k_2^{-1}=\tfrac{2}{3}k_b^{-1}+\frac{l_b^2}{12}k_\theta^{-1} \tag{32}$$

For isotactic polypropylene and polystyrene (in the diamond lattice approximation both lie on the same 3_1 helix):

$$k_1^{-1}=\tfrac{10}{9}k_\phi^{-1} \tag{33}$$

$$k_2^{-1}=\tfrac{10}{9}k_b^{-1}+\frac{4l_b^2}{9}k_\theta^{-1}+\frac{16l_b^2}{243}k_\phi^{-1} \tag{34}$$

For syndiotactic polypropylene:

$$k_1^{-1}=2k_\theta^{-1}+\tfrac{4}{3}k_\phi^{-1} \tag{35}$$

$$k_2^{-1}=\tfrac{4}{3}k_b^{-1}+\frac{l_b^2}{3}k_\theta^{-1}+\frac{8l_b^2}{9}k_\phi^{-1} \tag{36}$$

In the above, l_b is the bond length, equal to 1.54 Å. The following values for k_b, k_θ and k_ϕ, taken from the work of Shieh *et al.*[20], were used:

$$k_b=4.4\times10^{-11}\text{ erg Å}^{-2} \qquad k_\theta=0.8\times10^{-11}\text{ erg} \qquad k_\phi=0.131\times10^{-11}\text{ erg} \tag{37}$$

The values of k_1 and k_2 given in *Table 1* are then obtained.

Equations (17) and (28) take the form expected for the spring constant of an assembly of springs coupled in series, but with a contribution weighted by a geometrical factor proportional to the moment of the load borne by each spring. The net spring constant is influenced most strongly by the weakest springs in the assembly, so that, except in unusual cases, the torsional angles determine the spring constants. Polyethylene is one of these unusual cases. Because of the all-*trans* structure, elongational tensions are not borne by the torsional angles, but by the bond angles. This is obvious from equation (32), in which κ_ϕ is absent, or from equations (22) and (17), where $\boldsymbol{v}_i\times\boldsymbol{u}_i$ is normal to $\boldsymbol{e}_3$ for every bond in the chain. As a result, polyethylene has an unusually large value of k_2. Isotactic polypropylene is an intermediate case. One-half of the bonds in isotactic polypropylene lie parallel to $\boldsymbol{e}_3$; therefore $\boldsymbol{e}_3\cdot(\boldsymbol{v}_i\times\boldsymbol{u}_i)$ is zero for these bonds, and only one-half the torsional angles bear any load. The k_2 value for isotactic polypropylene lies between that of polyethylene and syndiotactic polypropylene, in which all the torsional angles cooperate in bearing the load. We shall see below that the range of k_2 values has important implications for the ability of the chain to transport solitons.

In contrast with k_2, torsional angles dominate in determining k_1 in all three cases, and the k_1 or k_1' values show much less variation. Angle bending contributions to k_1^{-1} would dominate only in the event that $v_{i3}=0$, i.e. only for bonds normal to the helical axis.

RESULTS OF THE SOLUTION OF THE EQUATIONS OF MOTION

The equations of motion, equations (10), were solved by a Newton–Raphson iterative procedure as discussed above. We only considered $\gamma_1^2=\gamma_2^2=1$ in these calculations, which formally represents the $v=0$, stationary, soliton. However, the $v=0$ energy is a lower bound to the energy of a moving soliton, and so is appropriate for comparison with experimental activation energies.

The initial estimate of the solution used in the Newton–Raphson procedure must be close to the true solution for the procedure to converge. To obtain a final structure we found it necessary to begin with a very short section of the chain (only 3–5 nodes). The initial structure of the short chain was taken as uniformly deformed with the two ends placed at different, symmetry-equivalent, minima of the $U'(x,\theta)$ function. With the two ends constrained to lie in the respective minima, convergence could be obtained

with no problems. The converged structure was then used as the starting point of a second calculation, adding one or several nodes at each end and constraining only the two outermost nodes. This procedure was repeated until eventually the chain became long enough that the distortion could support itself without constraints. The final structures achieved in each case were well relaxed, without constraints on any of the variables, and sufficiently long to have the tails on each end of the stem lying in essentially perfect crystallographic register.

The soliton energies reported below are given as relative to the perfect crystal structure. This generates some uncertainty in some cases, since, as noted in *Table 3*, the two minima spanned by the soliton do not have precisely equivalent energies, producing ambiguity in the value of the perfect-crystal energy to be used. The perfect-crystal energy used here is the simple arithmetic mean of the two minima, a logical choice given that the solutions always had solitons very near the centre of the stem. Nevertheless, some ambiguity, probably of the order of 0.1 kcal mol^{-1}, and smaller than errors due to other approximations, is present in the calculated energies of the two polypropylenes.

Our findings are summarized in the following paragraphs.

Soliton structures and energies

Polyethylene. The polyethylene potential (*Figure 2*) provides for a number of different solitons. The most stable solitons (labelled A and A′ in *Figure 7*), combining a 180° rotation and a $c/2$ translation, are the same as the structure calculated by Mansfield and Boyd[8] and are symmetry-equivalent enantiomers. Two other solitons (labelled B and C in *Figure 7*) both involve a translation of c and no net rotation, although during passage of soliton B the individual units rotate back and forth through approximately 90°.* The total computed energies of the three solitons A, B and C are 20.8, 36.7 and 25.7 kcal mol^{-1}, respectively. The energy of A is in good agreement with the experimental activation energy[24,25] of 17 kcal mol^{-1}, especially when one considers that our value should be high by about 3 kcal mol^{-1} because the surrounding stems were not permitted to relax[8].

The estimated energy of C is somewhat higher than A but close enough that both A and C might contribute to the mechanical α relaxation. However, only A contributes to the dielectric α relaxation since C produces no net rotation of the stem.

We attempted to obtain a soliton involving a complete 360° rotation with no net translation, but solutions always tended to degenerate to two individual solitons: A followed by A′ or vice versa. This is to be expected given the two peaks in $U'(x,\theta)$ that lie directly in the path of a pure 360° rotation. Net rotations through 360° are best achieved with two solitons.

Isotactic polypropylene. The soliton incorporating −120° rotation and $c/3$ translation (shown in *Figure 3*) was computed to have an energy of 38.2 kcal mol^{-1}. This is in reasonably good agreement with the experimental activation energy of the α relaxation, which is[26,27] 34.5 kcal mol^{-1}. It is evident from *Figure 3* that any other solitons that one might consider, e.g. a rotation through

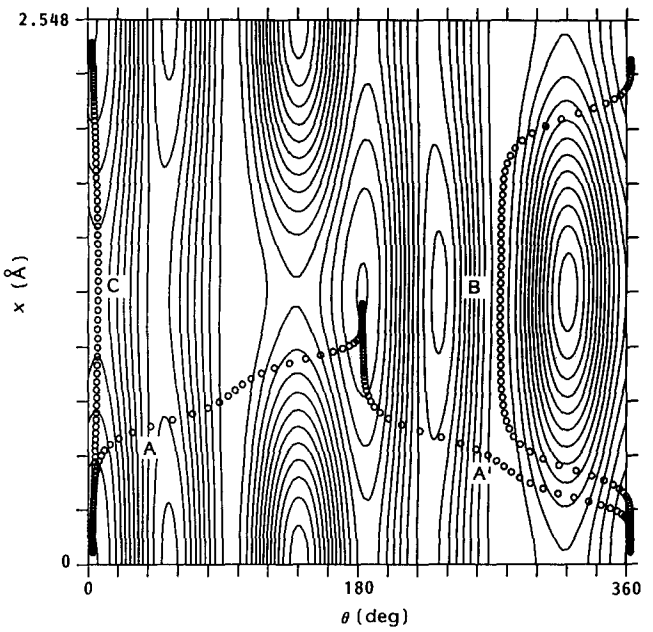

Figure 7 Same as *Figure 2*, but with soliton structures displayed

+120° and a translation through $2c/3$, or a rotation through +240° and a translation through $c/3$, would have energies considerably higher than this and need not be considered. Unlike polyethylene, this stem is chiral and can only support solitons of a given chirality.

Syndiotactic polypropylene. The only soliton meriting consideration in syndiotactic polypropylene is shown in *Figure 4* and is calculated to have an energy of 51.0 kcal mol^{-1}. No α relaxation has been observed in this polymer[16]. Such a large energy and other circumstances (to be discussed below) are consistent with the absence of the relaxation in this polymer.

Isotactic polystyrene. The lowest energy path between the minima in *Figure 5* passes through regions of several hundred kilocalories per mole. This is not apparent in *Figure 5*, since contours above 10 kcal mol^{-1} have been omitted. Such high energies are the result of steric overlap between phenyl groups and are adequate to explain the absence of the α relaxation in this polymer. Because of this, we felt it unnecessary to calculate a soliton in this particular case.

Crystal thickness dependence of activation energy; competition with rigid-rod motions in thin crystals

The strain field of the A, B and C solitons in polyethylene extend over about a hundred CH_2 units. In crystals thinner than this, the leading edge of the soliton is able to leave the crystal before the trailing edge has entered, with a resulting activation energy less than the thick-crystal value. This explains[8] the experimentally observed[24] crystal thickness dependence of the activation energy. We have estimated the activation energy as a function of crystal thickness for the A, B and C solitons in the following way. Starting with the well converged structures discussed above, we held the structure in place in the most highly distorted regions by constraining one or several nodes near the centre of the stem to lie at the same values of x and θ as in the long-stem calculation, and relaxed the structure with p and $K-p$ nodes, respectively, removed from the left and right ends of the stem. It was necessary to constrain the stem in this way since, without

*The possibility of the motion given by path B was suggested to the authors in a private conversation with Professor P. J. Barham. McCullough[22] also considers such motions.

long tails on either end of the strained portion of the stem, the soliton could not support itself and during the relaxation procedure would simply move off the end of the stem. At constant K with p varying, this calculation gives us the total strain energy in a stem of length $N = M - K$ as the soliton moves, where M is the length of the original structure. By taking the maximum strain energy obtained at each value of K, we are able to estimate the activation energy as a function of crystal thickness. *Figure 8* gives the results for the three polyethylene solitons.

Figure 8 also indicates that, in thin crystals, rigid-rod motions become competitive with the soliton motion. If the polymer stem moves rigidly, an activation energy proportional to the stem length is expected, with the proportionality constant being equal to the value of the energy $U'(x,\theta)$ at the saddle point through which the stem must pass. For rigid motions along the same general paths as solitons A, B and C, the saddle points lie at $(x,\theta) = (1.28, 46.9)$, (0, 318.6) and (1.27 Å, 6.5°), respectively, and require 0.94, 0.39 and 0.35 kcal mol^{-1}, respectively, for each CH_2 group in the stem. The activation energies for rigid-rod motions are shown as straight lines in *Figure 8*. These calculations predict that the favoured motion in stems of fewer than about 40 or 50

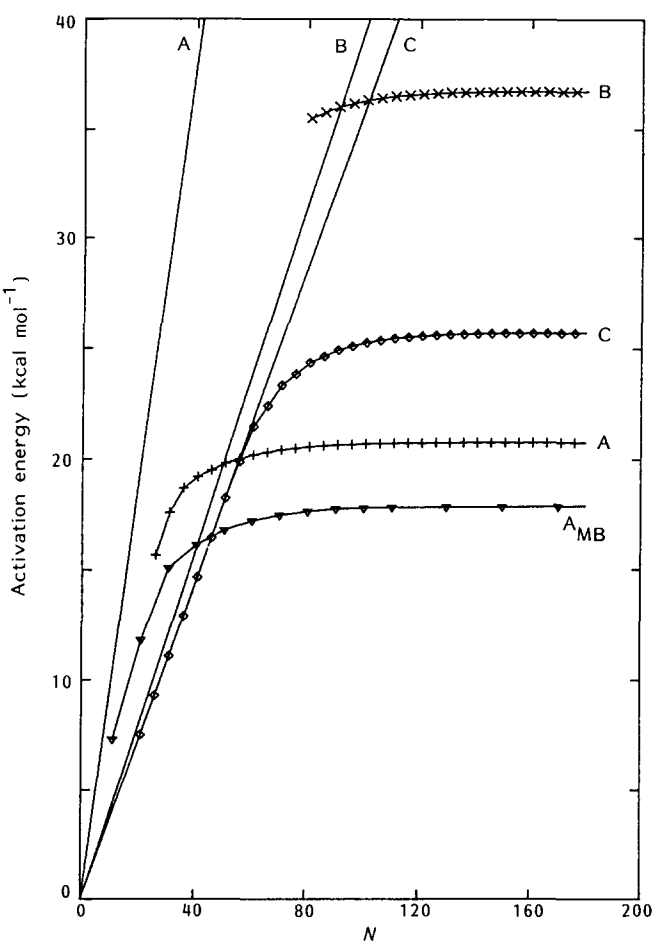

Figure 8 Activation energy as a function of crystal thickness for the three polyethylene solitons. N is the number of backbone atoms per stem. The curves labelled A, B and C give the activation energy for the A, B and C solitons, respectively, as calculated here. The curve labelled A_{MB} is the activation energy of soliton A as calculated in ref. 8. The three straight lines labelled A, B and C give the activation energy as a function of crystal thickness of rigid-rod motions following approximately the same paths as solitons A, B and C

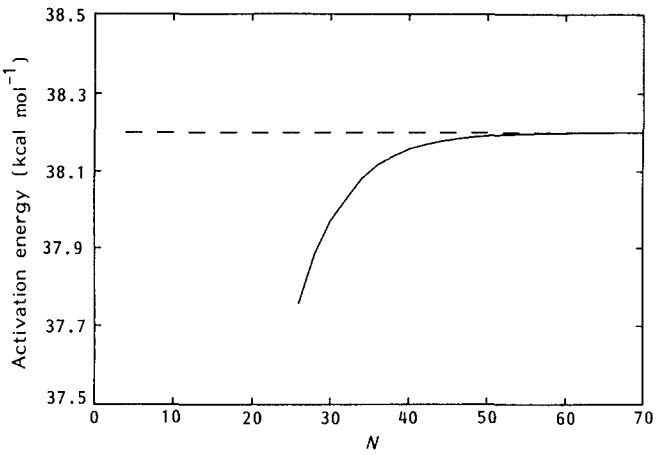

Figure 9 Activation energy as a function of crystal thickness for the isotactic polypropylene soliton. The broken line lies at 38.2 kcal mol^{-1} and represents the infinite-crystal limit

CH_2 groups is a rigid-rod translation along the chain axis occurring by two separate pathways, either a pure translation (path C) or a rotation through about −90°, followed by a translation, then by a rotation back through +90°.* These findings are in good agreement with experimental observations considering stem transport in paraffin crystals[28,29].

The translational motions B and C, rigid or not, are not expected to be dielectrically active. It appears then that the only dielectrically active motion is the A soliton, even in thin crystals, since the rigid-rod A motion always lies above the soliton in energy.

A similar calculation was performed for the isotactic polypropylene soliton, with results shown in *Figure 9*. Because isotactic polypropylene has a smaller k_2 value than polyethylene, it has a smaller strain field, and weaker crystal thickness dependence. The activation energy required for a rigid-rod motion, more than 3 kcal mol^{-1} per backbone atom, is so high that we can rule out the possibility of competition with rigid-rod motions in thin crystals.

Periodic barriers to soliton transport

As mentioned above, equations (1) are the equations of motion of a continuum model of a crystalline stem. A free-streaming soliton motion can only be expected in the limit in which the continuum model is valid. Since the polymer chain is actually discrete, we can expect that the soliton energy varies periodically as the soliton moves from one repeat unit to the next. Therefore, the soliton must traverse a series of energy barriers as it moves along the chain. If these barriers are large, soliton motion will occur as a sequence of thermally activated processes. Instead of streaming through the crystal, the soliton would perform a one-dimensional random walk. Any relaxation, if observed at all, would be much slower. Two effects, either large values of k_1 and k_2 or small values of $U(x,\theta)$, are expected to favour the continuum approximation. For the three polymers studied here, the k_1 values are roughly comparable, while the k_2 value of polyethylene is much larger than the k_2 values of the other polymers. In addition, the major features of $U(x,\theta)$ for polyethylene are about an order of magnitude smaller than those for either of the polypropylenes. The combined influence of these

* See previous footnote.

two effects makes polyethylene the most likely candidate for free-streaming soliton motion of the three polymers examined.

To understand better the effects of discreteness, we have attempted to estimate the barrier expected as the soliton moves down the chain. We are already solving a discretized form of the equations of motion (equations (10)) but, for this calculation to be correct, it is necessary for the discretization to coincide with the periodicity of the chain. This requires setting $h = l$ in equation (11), and such a value was used in this particular calculation. A well converged soliton structure was obtained, as described above. Those nodes at which the chain had the most strain were selected, and the soliton was made to advance one repeat unit by constraining those nodes to move in concert and continuously from their original position to the position of their next neighbour. The calculated change in strain energy is plotted in *Figure 10*. As expected, the barrier in polyethylene is smallest, calculated to be of the order of 1 cal mol^{-1} only, too small to be noticeable in *Figure 10*. Isotactic polypropylene exhibits a barrier of about 0.5 kcal mol^{-1}, and syndiotactic polypropylene a barrier of about 2 kcal mol^{-1}. The syndiotactic barrier is larger than kT and its value, combined with the value of the soliton energy itself (~ 50 kcal mol^{-1}), explains the absence of the α relaxation in syndiotactic polypropylene. The barrier of 0.5 kcal mol^{-1} in isotactic polypropylene undoubtedly contributes to soliton scattering, but is probably not so large that solitons moving down the stem have to be thermally activated at each step. The barrier in polyethylene is very small, and so is not expected to contribute appreciably to soliton scattering in these systems.

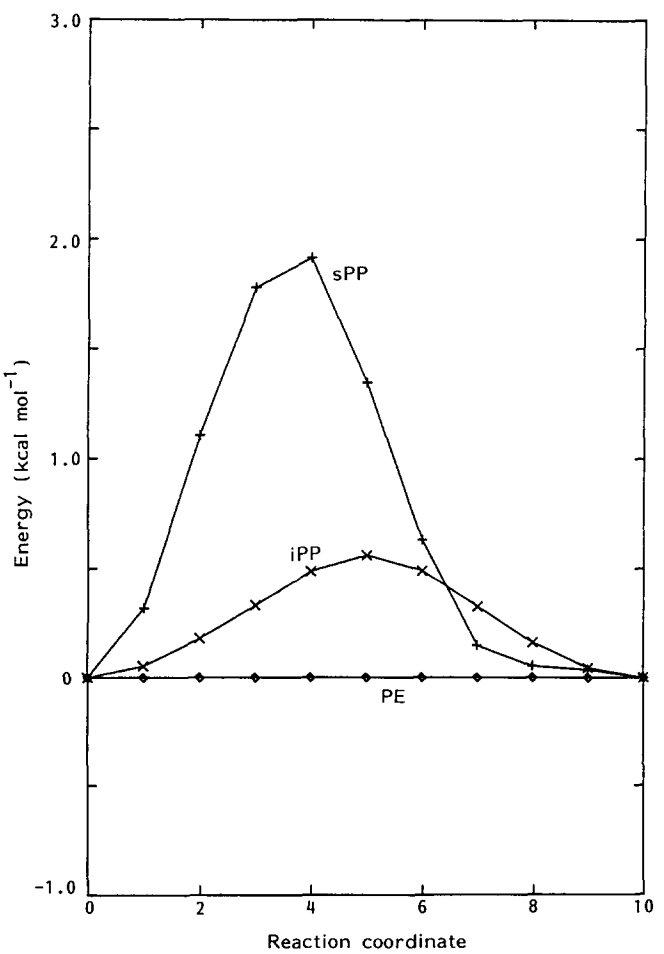

Figure 10 Periodic energy barriers to soliton transport. The solitons in each of the three polymers, polyethylene (PE), isotactic polypropylene (iPP) and syndiotactic polypropylene (sPP), must surmount the energy barriers shown here to move one repeat unit in the lattice

DISCUSSION AND SUMMARY

The soliton model successfully predicts the presence or absence of an α relaxation in the four polymers studied, namely polyethylene, isotactic and syndiotactic polypropylene, and isotactic polystyrene. It successfully predicts the activation energy of the relaxation for the two polymers, polyethylene and isotactic polypropylene, that exhibit the relaxation. As a result of these calculations, a number of general rules controlling the presence of the α relaxation can be given. These are summarized below.

(1) The interstem potential energy function $U'(x,\theta)$ should provide easy pathways between minima. The saddle points in polyethylene, isotactic polypropylene and syndiotactic polypropylene are all below 4 kcal mol^{-1} per backbone atom, but are much larger in isotactic polystyrene. Given this, there is little wonder that isotactic polystyrene does not have the α relaxation. In the case of the hydrocarbon polymers studied here, the features of the $U(x,\theta)$ function are determined by the presence or absence of bulky side groups. Isotactic polystyrene, with its pendant phenyl groups, has a much higher saddle point than either of the polypropylenes that bear methyl groups, and these in turn have higher saddle points than polyethylene. Specific interchain interactions, such as dipole–dipole interactions or hydrogen bonding, should also contribute to higher saddle points in the $U(x,\theta)$ function. Smaller features in the $U(x,\theta)$ function also favour smaller periodic barriers to soliton transport as the soliton moves from one repeat unit to the next.

(2) The spring constant k_2 should be large, but not too large. A small k_2 would tend to decrease the total activation energy; but, if it is too small, large periodic barriers to soliton transport from one repeat unit to the next will result. Too large a k_2 would give too large an activation energy. The point at which k_2 becomes too large depends on the $U'(x,\theta)$ function. The geometrical structure of the chain appears to be the strongest factor affecting the value of k_2. Geometrical structures in which the bulk of any elongational load is borne by the bond-bending degrees of freedom yield higher values of k_2. All-*trans* chains are the best examples of this, yielding the largest values of k_2. Everything that we have said about the influence of k_2 on the α relaxation would probably also apply to k_1; however, k_1 values are not expected to vary so widely from one polymer to another.

(3) The number of bonds per repeat unit should be small. The soliton has to incorporate enough accumulated strain to account for an excess or a lack of one repeat unit. Clearly, this is easier if the repeat unit is shorter. The two polypropylenes are a good example of this effect. The saddle points in $U'(x,\theta)$ for the two polymers both lie at about 3 kcal mol^{-1} per backbone atom, but the activation energy of isotactic polypropylene, with two backbone bonds per repeat unit, is predicted to be considerably lower than that of syndiotactic polypropylene, with four backbone bonds per repeat unit.

Most of the above rules have been conjectured previously[9,15]. Our calculations confirm these conjectures.

On the basis of the above rules, we are able to explain the presence of an α relaxation in polymers such as polytetrafluoroethylene, polyoxymethylene, poly(ethylene oxide) or poly(vinyl fluoride), and the absence of an α relaxation in polymers such as the nylons or polyesters. The former have simple repeat units and many crystallize in all-*trans* or nearly all-*trans* structures, while the nylons and polyesters have long repeat units and are expected to have large features on the $U'(x,\theta)$ function, since rotation or translation of a stem would require breaking of hydrogen bonds or dipole–dipole interactions.

These calculations also permit us to say something about the expected crystal thickness dependence of the α relaxation. Two effects can be cited. One is the change in activation energy with crystal thickness that is observed when the crystal thickness is smaller than the strain field of the soliton. The other is the effect of a periodic barrier to soliton transport as the soliton progresses from one repeat unit to the next. The latter effect is only expected to affect the prefactor of the rate expression, but in extreme cases it can probably produce a considerable slowing of the rate. This effect is expected to be crystal-thickness-dependent since the series of barriers will contribute to soliton scattering, and soliton back-scattering would become more important as the crystal thickness increases.

As a result of these calculations, we are also able to predict that two different modes of rigid-rod chain translation are the preferred motions in thin polyethylene or paraffin crystals, although these motions do not contribute to the dielectric relaxation. The two modes are, first, a pure translation through two CH_2 groups and, secondly, a rotation through 90° in one direction followed by a translation through two CH_2 groups followed by a 90° rotation in the reverse direction. The dielectric relaxation in all polyethylene crystals, thick or thin, is dominated by the passage of solitons combining 180° rotation and translation through one CH_2 group, as is the mechanical relaxation of thick crystals.

ACKNOWLEDGEMENTS

Acknowledgement is made to the donors of the Petroleum Research Fund, administered by the American Chemical Society, for partial support of this work. Partial support was also provided by the National Science Foundation, Grant Nos. DMR-8451928 and DMR-8607708.

REFERENCES

1 Frölich, H. *Proc. Phys. Soc. Lond.* 1942, **54**, 422
2 Frölich, H. 'Theory of Dielectrics', 2nd Edn., Oxford University Press, Oxford, 1958
3 Tuijnman, C. A. F. *Polymer* 1963, **4**, 259
4 Tuijnman, C. A. F. *Polymer* 1963, **4**, 315
5 Hoffman, J. D., Williams, G. and Passaglia, E. *J. Polym. Sci. (C)* 1966, **14**, 173
6 Booij, H. C. *J. Polym. Sci. (C)* 1967, **16**, 1761
7 Williams, G., Lauritzen, J. I. and Hoffman, J. D. *J. Appl. Phys.* 1967, **38**, 4203
8 Mansfield, M. and Boyd, R. H. *J. Polym. Sci., Polym. Phys. Edn.* 1978, **16**, 1227
9 Mansfield, M. L. *Chem. Phys. Lett.* 1980, **69**, 383
10 Skinner, J. L. and Wolynes, P. G. *J. Chem. Phys.* 1980, **73**, 4015
11 Skinner, J. L. and Wolynes, P. G. *J. Chem. Phys.* 1980, **73**, 4022
12 Scott, A. C., Chu, F. Y. F. and McLaughlin, P. W. *Proc. IEEE* 1973, **61**, 1443
13 Skinner, J. L. and Park, Y. H. *Macromolecules* 1984, **17**, 1735
14 Boyd, R. H. *Polymer* 1985, **26**, 323
15 Boyd, R. H. *Polymer* 1985, **26**, 1123
16 Aharoni, S. M. and Sibilia, J. P. *Polym. Eng. Sci.* 1979, **19**, 450
17 Reneker, D. H. *J. Polym. Sci.* 1962, **59**, 539
18 Reneker, D. H. and Mazur, J. *Polymer* 1982, **23**, 401
19 Natta, G. and Danusso, F. 'Stereoregular Polymers and Stereospecific Polymerizations', Pergamon Press, Oxford, Vol. 2, 1967
20 Shieh, C. F., McNally, D. and Boyd, R. H. *Tetrahedron* 1969, **25**, 3653
21 Syi, J.-L. Doctoral Dissertation, University of Maryland at College Park, 1986
22 McCullough, R. L. *J. Macromol. Sci.–Phys. (B)* 1974, **9**, 97
23 Mansfield, M. L. *J. Chem. Phys.* 1980, **72**, 3923
24 Ashcraft, C. R. and Boyd, R. H. *J. Polym. Sci., Polym. Phys. Edn.* 1976, **14**, 2153
25 Sayre, J. A., Swanson, S. R. and Boyd, R. H. *J. Polym. Sci., Polym. Phys. Edn.* 1978, **16**, 1739
26 McCrum, N. G. and Pizzoli, M. *J. Mater. Sci. Lett.* 1977, **12**, 1920
27 McCrum, N. G. *J. Mater. Sci. Lett.* 1978, **13**, 1596
28 Ungar, G. and Keller, A. *Colloid Polym. Sci.* 1979, **257**, 90
29 Zerbi, G., Piazza, R. and Holland-Mortiz, K. *Polymer* 1982, **23**, 1921